



Modeling Wind Speed with a Long-Term Horizon and High-Time Interval with a Hybrid Fourier-Neural Network Model

Juan Gabriel Rueda-Bayona^{1*}, Juan José Cabello Eras², Alexis Sagastume Gutiérrez²

¹ Engineering Faculty, Civil Engineering, Water and Energy (AyE), Research Group, Universidad Militar Nueva Granada, 111071, Colombia

² Energy Department, Universidad de la Costa, Barranquilla 080002, Colombia

Corresponding Author Email: juan.rueda@unimilitar.edu.co

<https://doi.org/10.18280/mmep.080313>

ABSTRACT

Received: 11 March 2021

Accepted: 18 May 2021

Keywords:

Fourier analysis, nonlinear autoregressive network, wind potential, reanalysis, wind-speed

The limited availability of local climatological stations and the limitations to predict the wind speed (WS) accurately are significant barriers to the expansion of wind energy (WE) projects worldwide. A methodology to forecast accurately the WS at the local scale can be used to overcome these barriers. This study proposes a methodology to forecast the WS with high-resolution and long-term horizons, which combines a Fourier model and a nonlinear autoregressive network (NAR). Given the nonlinearities of the WS variations, a NAR model is used to forecast the WS based on the variability identified with the Fourier analysis. The NAR modelled successfully 1.7 years of wind-speed with 3 hours of the time interval, what may be considered the longest forecasting horizon with high resolution at the moment.

1. INTRODUCTION

Renewable energy applications have been growing in the last two decades as a result of policies and strategies to mitigate climatic change, and it is currently growing faster than other energy sources [1]. In particular, the generation of electricity is one main emitter of greenhouse gases (GHG), accounting for around 25% of global emissions [2]. Electricity generation is one main application of RES [3]. The use of RES supported 24% of the global electricity demand in 2016, while it is forecasted that in 2030 it will support some 30% [4].

Worldwide, wind energy (WE) follows hydroelectric energy as the most widespread RES, which is explained because of its technological maturity [5], environmental advantages [6], and lower costs as compared to other RES [7]. In emerging economies like China, there is an increasing trend to invest in WE (i.e. inland and offshore applications), accounting for 87 % of the investments in RES [8]. Currently, there is a need to research further to identify areas with high WE potential, which in practice will require to forecast accurately the WS with a long-term horizon and high-time interval resolution [9].

The electricity output of wind turbines largely depends on the weather conditions and their natural variability [10]. Forecasting the electricity production of wind farms (WF) based on the weather forecast is one of the main challenges to deliver large amounts of wind-based electricity to electric grids [11]. Since electric grids must guarantee a stable service regardless of the variability of the WS, forecasting the performance of wind turbines is critical [4, 12], which depends on the WS [13]. Forecasting the electricity output of (WF) during its exploitation is a cornerstone for costs/benefits assessment, electricity dispatch planning [14], optimizing operational parameters and the performance of wind turbines [15], and optimizing the load balancing [14]. Furthermore, it

is essential for the adequate selection of WFs location and their capacity planning [16]. Frequently, the electricity output of wind turbines is forecasted using a fixed-weighted measure of its nominal generation capacity, and historic atmospheric data [17].

Forecasting the WS has been widely investigated [18], and several models with probabilistic approaches [19] or methods considering different time horizons are available in the specialized literature [20-23]. However, given its insufficient accuracy, there is a need to develop new approaches [11]. The lack of meteorological data and local climatological stations make in difficulties to locally forecast the WS with adequate accuracy [24]. Particularly, in Colombia, the limitations to accurately predict the WS are one main barrier to expand the implementation of WE projects [25].

Therefore, this research coupled a Fourier model and a Autoregressive Neural Network to forecast the WS at the local scale with a long-term horizon and high-time interval, for locations with limited or no availability of meteorological data. To overcome the lack of data in locations without meteorological stations, data from the North American Regional Reanalysis (NARR) is used [26].

1.1 Literature review

There are different time horizons to forecast the WS [27]:

- Very short-term: ≤ 30 min [28].
- Short-term: 30 min \div 6 hours.
- Medium-term: 6 hours \div 1 day.
- Long-term: > 1 day [29].

Another classification was proposed for the time horizons [30]:

- Immediate-short-term (hourly periods and less than a

day).

- Short-term forecasting (next day).
- long-term forecasting (several days in the future).

Using numerical modeling and in-situ data assimilation, three models with a resolution at the mesoscale and the microscale were developed to assess the wind energy potential in two different locations [31]. The results show that neither the mesoscale nor the mesoscale-microscale models are applicable at local scales. Another, model non-hydrostatic primitive equations (MM5) were used to generate a wind atlas over Greece for a typical year, to estimate the national WE potential [32]. Using the kernel density estimation model (KDE) the WE of 10,698 meteorological stations in China were assessed [33]. In this case, the daily average of the WS was forecasted for 5 years (2010-2014). Moreover, statistical models like the autoregressive conditional heteroskedasticity and the autoregressive integrated moving average were implemented to assess the hourly fluctuations of the WS in WE applications [34]. In a different study, a multi-step

forecast of the WS with a 4 days horizon was developed with a hybrid scheme [35]; the scheme integrated the physical weather model (WRF) (wrf-model.org), a novel fuzzy logic system, and the Cuckoo search optimization. This hybrid model was used to forecast the WS for 96 points considering a short-term horizon. However, results show that the higher horizontal resolution not always ensure high precision. A different hybrid model (ie. hybrid machine intelligent SVR) was used to assess the WS and the resulting WE for the immediate-short-term horizon in four WF locations in different countries [36]. The results show that the WS forecasting was improved for short term periods of wind events.

To forecast WS for short-term horizons, other studies use a linear fuzzy neural network [37], multivariate autoregressive moving average model [38], and wavelet transforms with the convolutional neural network [30], which is strongly recommended for short-term horizon [39-42]. In particular, support vector machine (SVM) models have good results forecasting WS for short-term horizon [43].

Table 1. AI techniques to forecast the WS with high time interval resolution

Method	Comments
Locally recurrent neural network [44]	TH – 72 h TI – 1 h Uses of 3 learning algorithms: Decoupled RPE, Neuron Linear Model RPE, and Neuron Non-linear Model RPE.
Ridgelet neural network (RNN) [45]	TH – 29 days TI – 1 h Uses differential evolution algorithm including a novel operator to forecast the WS.
Elman neural network [46]	TH – 3h TI – 30 min An artificial neural network is combined with an adaptive Bayesian learning procedure and a Gaussian approximation process.
Nonlinear autoregressive network with exogenous inputs (NARX) [47]	TH – 1 year TI – 1 h Use of two-layer feed-forward backpropagation networks, with 6 and 30 neurons in the middle and output layers.
No negative constraint theory (NNCT) integrated with the AI methods [48]	TH – 10.4 days TI–1 h Combines the no negative constraint theory (NNCT) with AI methods
Extreme Learning Machine (ELM), Ljung-Box Q-test (LBQ) and Auto-Regressive Integrated Moving Average (SARIMA) [49]	TH–63 days TI – 1 day The extreme learning machine (ELM) is combined with the Ljung-Box Q-test (LBQ), and the Auto-Regressive Integrated Moving Average (SARIMA)
Discrete-time Markov chain models [50]	TH –2 h TI – 10 min Independent evaluation of a first and a second-order Markov chain model.
Secondary Decomposition Algorithm (SDA) and the Elman neural network [51]	TH –1 day TI – 30 min To forecast the WS, the wavelet packet decomposition (WPD) is combined with the fast ensemble empirical mode decomposition (FEEMD) to filter the Elman neural networks.
Multi-objective differential evolution (MODE) algorithm [52]	TH – 7.08 days TI – 1h Optimization of multiple contradictory objectives, using the MODE algorithm combined with an SVM and the LUBE method.
Extreme Learning Machine (ELM) [53]	TH – 6h TI – 1h Use of a bidirectional mechanism and a backward ELM network.
Machine learning methods (MLM) [15]	TH – 6 days TI – 10 min Use of 5 MLM strategies (Recursive, Direct, DirRec, MIMO, DIRMO), and 3 strategies derived from the simple transformation of the MIMO and DIRMO approaches.
Non-linear autoregressive (exogenous) model (NAR) [54]	TH – 1 day TI – 1 hour Use of a general regression neural network GRNN (ARIMA), which identify the results, and a Fibonacci search method.
Artificial neural network (ANN) and support vector machine (SVM) [55]	TH – 31 days TI – 1 hour Use of empirical mode decomposition (EMD) for signal decomposition to facilitate the forecasting with ANN and SVM.
Backpropagation Neural Network (BP-NN) [56]	TH – 11.04 days TI – 1 hour Signal filtering using an empirical mode decomposition (EMD), combined with the BP-NN integrated with a Genetic Algorithm to forecast the WS
Linear and a nonlinear autoregressive moving average model with exogenous inputs (ARMAX) [57]	TH – 1 day TI – 1 hour Use of ARMAX techniques, including the linear, SMOreg (based in an SVM), the Bagging algorithm, and the M5R algorithm.
Machine Learning Technique. [58]	TH – 6.25 days TI – 1 hour Use of a two-layer MLT system with a data-driven multi-model.
Neuro-fuzzy inference system (ANFIS) [59]	TH – 2,6,12 h TI – 1 h Use of the Pearson correlation coefficient to preprocesses the data, and, afterward, application of three individual forecasting models: BP-NN, radial basis function neural network (RBF-NN) and least squares support vector machine (LSSVM) in the ANFIS system.
Back propagation Neural Network (BPNN) combined with discrete wavelet transform (DWT) and brain storm optimization (BSO) [60]	TH – 7 days TI – 10 min Use of 10 - 12 hidden layers of wind speed for training. The model applies the DWT for removing the noises, then, the BSO selects optimal parameters for the BPNN.

Charged

Search System Algorithm (CSSA) integrated with a Lower Upper Boundary Approximation (LUBA) neural network

Use of the Numeral Weather Prediction (NWP) data to train the CSSA-LUBA model.

TH - Time horizon TI - Time interval

Table 1 shows different applications of artificial intelligence (AI) techniques used to forecast the WS for high time interval resolution.

Table 1 shows that to forecast the WS at the local scale, data is used to train the networks of artificial intelligence methods, which come from in-situ measured time series during less than 30 years. Additionally, the longer time horizon considered to forecast the WS is one year. Most of the artificial intelligence and stochastic methods used to forecast the WS needed a filtering or signal decomposition step to reduce the non-linearities of the input training data used.

2. METHODOLOGY

This study combines the Fourier analysis with a nonlinear autoregressive network to forecast the WS at the local scale. Commonly, the programmer must transform the NAR neural network to a close loop for the multistep-ahead prediction [59], however, this study used the open loop mode with target (input) data generated by a Fourier model for the multistep-ahead prediction.

2.1 Fourier analysis

Harmonic analysis decomposes time series in either harmonics or regular waves with specified parameters to identify the natural oscillations of climate variables. The use of the Fourier coefficients in the real-time series is the sum of its harmonic waves:

$$y(t_n) = \frac{a_0}{2} + \sum_{k=1}^M a_k \cdot \cos(\omega_k t_n) + b_k \cdot \sin(\omega_k t_n) \quad (1)$$

In this case, the time (t_n) and the angular frequency (ω_n) are calculated as:

$$t_n = n \cdot \Delta t \quad (2)$$

$$\omega_n = 2 \cdot \pi \cdot \frac{k}{N} = 2 \cdot \pi \cdot f_k \quad (3)$$

where, k is the harmonic, ω_n Angular frequency, k is the k -th harmonic, M the number of identified harmonics, Δt time interval, n number of observations in the time series.

Then, the minimum value of the frequency is calculated as:

$$k = 1 \rightarrow f_0 = \frac{1}{N} \rightarrow \omega_1 = \frac{2 \cdot \pi}{N} \quad (4)$$

The minimum value of the frequency (maximum period) that could be within the dynamics of the time series depends of the length of dataset. Hence, it is recommended for wind speed modelling through Fourier analysis, that time series gathers the natural variability of the parameter, e.g climate

variability events such as Pacific Decadal Oscillations which have approximately 10 years of period [62]. In this sense, this study recommends using datasets of WS \Rightarrow 10 years, to consider this natural cycle in the calculations of the Fourier coefficients.

Moreover, to calculate the maximum frequency is considered that $f_0 \leq f \leq f_M$:

$$k = M \rightarrow f_M = \frac{1}{2 \cdot \Delta t} \rightarrow \omega_1 = \frac{\pi}{\Delta t}, M = \frac{N}{2} \quad (5)$$

The Fourier coefficients are determined as:

$$a_0 = \frac{2}{N} + \sum_{n=1}^M y(t_n) \quad (6)$$

$$a_k = \frac{2}{N} + \sum_{n=1}^N y(t_n) \cdot \cos(\omega_k t_n) \quad (7)$$

$$a_{N/2} = \frac{1}{N} + \sum_{n=1}^N y(t_n) \cdot \cos(\pi \cdot t_n) \quad (8)$$

$$b_k = \frac{2}{N} + \sum_{n=1}^N y(t_n) \cdot \sin(\omega_k \cdot t_n) \quad (9)$$

The amplitude of each harmonic is calculated as:

$$c_k^2 = a_k^2 + b_k^2 \quad (10)$$

The phase of each harmonic is:

$$\theta_k = \tan^{-1} \frac{b_k}{a_k} \quad (11)$$

Then, the signal is calculated as:

$$y(t_n) = \frac{C_0}{2} + \sum_{k=1}^M C_k \cdot \cos(\omega_k t_n - \theta_k) \quad (12)$$

The signal is the Fourier modelled time series, and its precision for simulating the raw time series depends on the number of selected harmonics for the $y(t_n)$ calculation (12). When calculating the Fourier parameters for long time series, computational restrictions could appear because of software-hardware limitations. Therefore, to avoid the computational restrictions such as out of memory, the identification of main harmonics through a spectral analysis (wind periodograms) may reduce the number of computational operations. This study recommends comparing the $y(t_n)$ calculated with all the harmonics against a $y(t_n)$ calculated with the most energetic harmonics (k_e). These k_e can be identified with the more

distinctive amplitudes in the periodogram. The final number of selected harmonics will depend of the accuracy of the Fourier model for simulating the raw data and the capability of the computer for handling the intense CPU-RAM processes.

Because of its lower computational requirements, the fast Fourier transform (FFT) is used for the Fourier analysis to compute the discrete Fourier transform (DFT). Thus, the numerical series is transformed from the time domain into a signal with a frequency domain. The FFT solves polynomial multiplication, filtering algorithms, differential equations, etc. [60, 61]. The mathematical basis of the FFT and DFT are discussed in the literature [63, 64]. The main issue of FFT is the Gibbs-Wilbraham phenomenon, introducing jumps discontinuity in the decomposition of discontinuous functions into cosine and sine waves finite series. On occasions, the Gibbs-Wilbraham phenomenon results in an overshoot of the convergence of the partial sum when a function is expanded [65]. Some approaches to addressing the Gibb-Wilbraham phenomenon includes the application of either a continuous wavelet [66] or a discrete wavelet [67] transforms.

2.2 Nonlinear autoregressive network (NAR)

The NAR model is an artificial neural network, including inputs from time series $y(t)$, weights (w), bias (b), hidden layers (k), and outputs $y(t)$ [68]. The inputs-outputs $y(t)$ are signals that each neuron receives and sends, and its synaptic activity depended of the weights, which are considered as a synaptic efficacy that excite ($w > 0$) or inhibit ($w < 0$) the neuron response. In this sense, when setting the weights values, assigning positive w will activate the neuron and negative values will inhibit it. The hidden layers are the half of neurons utilized in the input and output layers, and there is no a general criterion for assigning the number of hidden layers, however, a performance assessment of the NAR model could reveal if hidden layers would be necessary.

During the training process of the NAR model, the initial w values could be equal to 1, however, the weight values can be assigned aleatory to explore a better fit of the expected results. Assigning high η (Learning rate) imply that w will have a high change each cycle of training (epoch), contrary to assigning η values below of 0.25, what provoke low changes over the w . Low η values represent a slow adjustment of w values easing a more precise adjustment of the model, but too low η must be avoided because it could provoke that model falls in local minima and clog. Because it is expected that NAR model mimics the target data with the most feasible precision, the η of this study was 0.25, that represents that 25 % of the input data will be used for training the NAR model.

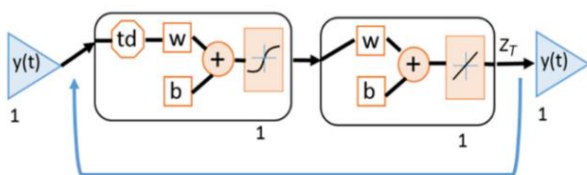


Figure 1. NAR configuration in open loop mode

The NAR includes the dynamic back response using the output time series as input during the network training, which increases the learning rate (η) of the perceptrons. Additionally, the NAR introduces a time delay (td) that supply some past predictions, thus improving its autocorrelation and covariance:

$$y(t+h) = f(y(t-1), \dots, y(t-td)) \quad (13)$$

where, h is the forecasting time horizon. As reference, a previous model configuration performed by the authors [24] was considered and is depicted in Figure 1.

In this case, a hidden layer uses a sigmoid function to activate weights and a linear equation is used in the output layer validation. The input data is feed to the NAR considering the output results. The backpropagation method is used to update the weights with consecutive forward and backward steps, and the bias (b) may be known as the effect of applying a transformation of the weighted sum. The net_i is constructed according to Eq. (12):

$$net_i = \sum w_{kj} \cdot y_j \cdot b \quad (14)$$

The NAR validates the partial results (z_j) with a sigmoid function:

$$z_j = \frac{1}{(1 + e^{-net_i})} \quad (15)$$

If the partial results are accurate, they are selected.

Before the finish of the forward step, the total or partial net_i is determined to calculate the error:

$$z_t = \sum w_{kj} \cdot z_j \quad (16)$$

$$error_i = 1 - z_t \quad (17)$$

The forward step ends when the error is smaller than the admissible value defined. Then, the backward propagation starts, assessing the output gradients and hidden layers with a local gradient (δ_j):

$$\delta_j = error_i \cdot z_j \cdot (1 - z_j) \quad (18)$$

$$\delta_i = \sum \delta_j \cdot w_{kj} \cdot z_j \cdot (1 - z_j) \quad (19)$$

Then, the local gradient was backward propagated along the network using the Delta rule [69], then the NAR stops until recalculated weights meet the user criterium. The Delta rule is considered a gradient descent learning rule that allows to updating the w values of single-layer neural networks every training cycle (epoch), then, the Delta rule is a mechanism that add or subtract the error magnitude to the w values till the model reach a suitable adjustment. Hence, the weights are recalculated using the Delta rule:

$$\Delta w_{kj} = \eta \cdot \delta_i \cdot z_i \quad (20)$$

Finally, the new weights are calculated:

$$w_{kj} = w_{kj} + \Delta w_{kj} \quad (21)$$

The NAR is used to define parameters to predict the time series, including the number of layers, the weights, and the biases. Figure 2 shows the methodology used in this study.

Step 1 initiates by extracting the WS data available from NARR for the specific location to be studied, then the data time series are extracted. Following, during the climate

variability analysis (step 2) the natural variations and oscillations are identified in a periodogram (i.e. step 2a). Furthermore, in step 2b (Figure 2), the Fourier parameters selected in step 2a are used to model the WS. Afterward, the Reanalysis data is used to train and validate the artificial neural network.

The data model combined with the Fourier transforms are used as input-target to predict the WS (step 3a). Then, linear regression (scatter plot) is developed in step 3b to evaluate the quality of the Hybrid Fourier-NAR modeled data by comparing it to the in situ data extracted from NARR (raw data). The scatter plot shows how the data raw-modelled ratio is distributed and the ratio direction-strength between the independent (raw data), and the dependent values (modelled data). Accordingly, a normally distributed ratio, with positive correlation coefficient ($r > 0.7$) and a low Root Mean Squared Error (RMSE) will ease the performance assessment of the Hybrid Fourier-NAR model. The pseudo code of the Hybrid Fourier-NAR model (Figure 2) is shown next:

READ Reanalysis data
DETERMINE one location (pixel) of the study area
EXTRACT time series
COMPUTE Fourier model parameters
DISPLAY periodogram
DO spectral analysis
SET Fourier parameters (amplitude, phase, frequency) and

time horizon (e.g 10 years).

SUM Fourier harmonics to obtain modelled time series.

COMPARE the modelled and raw time series.

EXTRACT 1-2 years from the modelled time series

ADD Fourier modelled time series at the end of the Reanalysis time series (combined time series).

INITIALIZE the NAR model.

READ input data (combined time series)

SET neural network parameters (w, b, layers, input-outputs).

TRAIN the NAR model with $\eta = 0.25$ in open loop mode.

VALIDATE NAR modelled data against raw data (input data).

CALCULATE statistical parameters (r-correlation, RMSE) for validation and performance assessment of the NAR model (error histogram, epochs).

IF statistical parameters don't meet the user requirements

SET new neural network parameters (w, b, layers, input-outputs).

ELSE remove trends in Fourier modelled time series

TRAIN the NAR model with $\eta = 0.25$ in open loop mode.

VALIDATE NAR modelled data against raw data (input data).

CALCULATE statistical parameters (r-correlation, RMSE), for validation and performance assessment of the NAR model (error histogram, epochs).

END

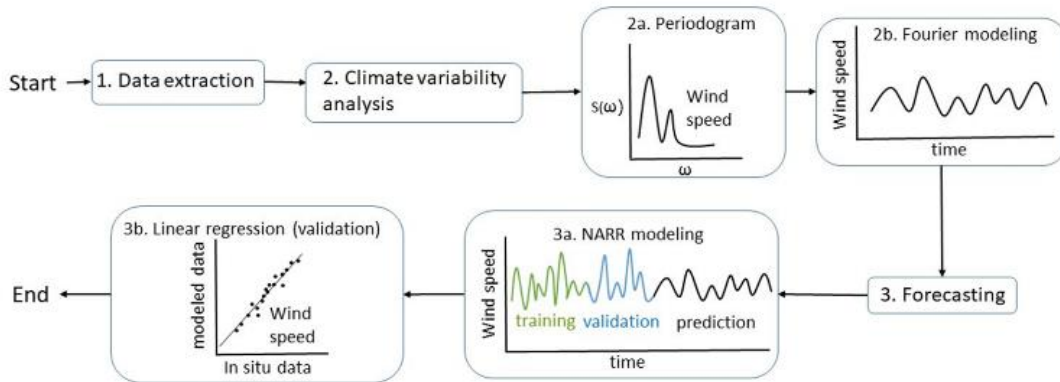


Figure 2. Wind forecasting methodology

3. RESULTS AND DISCUSSION

The method described in Figure 2 was used to forecast the WS in Barranquilla (Colombia).

3.1 Data extraction

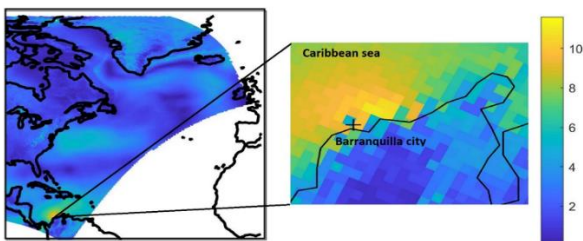


Figure 3. Wind speed data from the NARR database for Barranquilla (Colombia)

The WS data from the NARR database was extracted from one pixel for the period defined [70]. Figure 3 shows a snapshot of Barranquilla in NARR.

The cross (+) indicates the coordinates of the selected pixel (i.e. 11.101637 N and 74.767269 W). The NARR database has been measuring the WS since January 1st, 1979. Data is measured with 0.3 degrees of spatial resolution (i.e. 32 km), for time intervals of three hours. In this study, data between 1979 and 2017 (i.e. over 30 years of data) was used for the climate variability analysis.

3.2 Identification of natural variability

Figure 4 shows the periodogram generated with the Fourier analysis.

The climatic variability occurs at different durations, for example, sea-breeze varies within the day, while there are seasonal (5.5 months) and annual (10.9 months) variabilities. Other effects vary in longer periods in the amplitude of the WS

natural cycles, the effects of ‘El Niño’ varies in 5.39 years, while and the Pacific Decadal Oscillation varies in 11.08 years. A simulation of 10.27 years time horizon with 30,000 values of the WS at 3 hours of the time interval, was developed using the Fourier model for Barranquilla, Colombia (Figure 5).

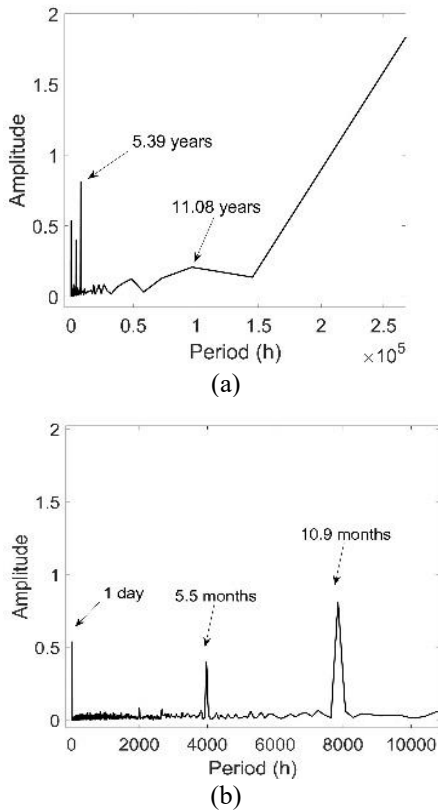


Figure 4. Wind speed periodogram for Barranquilla (Colombia). a) Periodogram (1979 – 2017) b) Zoomed periodogram for around 1 year

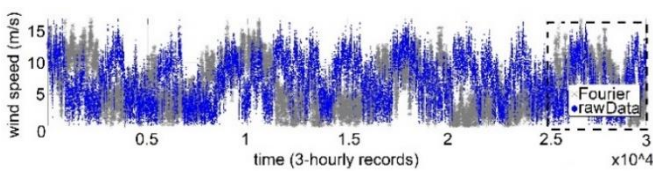


Figure 5. Wind speed for 10.27 years of time horizon in Barranquilla (period: from 01:00 h of 01-01-1979 to 02:00 h of 27-02-1990)

The results show that the oscillation modeled from Fourier analysis follows the trend of the measured data, although for some periods the accuracy was under the standards defined. Then, the Fourier model was validated with a scattering analysis by correlating the raw data (i.e. the 30,000 measures used) and the model results. The resulting correlation is low (i.e. $R^2 = 0.22$). These results show that, given the non-linearities of climate variability, the Fourier model cannot be used for the accurate simulation of the WS variations for long time horizons. However, the scattering analysis was developed for a time horizon of around 1 year, resulting in higher correlations (i.e. R^2 varied between 0.6 and 0.7), which is adequate for input data in the NAR model. A time horizon of 1.71 years (dash-line rectangle in Figure 5) was considered in the Fourier model to generate the input data used in the NAR model.

3.3 Forecasting the wind speed

MATLAB software was used, and different neuronal network designs were tested for the NAR model of Barranquilla. The neuronal network design of one hidden layer and three delays showed the best results. Data obtained from the Fourier analysis was feed to the NAR model, to consider the non-linearities of the WS. The NAR was trained and calibrated using the data from the 10.27 years at 3 hours of time intervals (Figure 6), what correspond to a time period between 00:00 h of 01-01-1979 year to 03:00 hr 27-02-1990 year. This data was also used to validate de forecasted data. The first 25 % of the data (i.e. 7500 values) were used to train the NAR, while the second 25 % (7500 records) of the data was utilized to validate the NAR. Finally, the remaining 50% (i.e. 15000 measures) were used to validate the results. Considering that NAR models mimic the inputs data, this study replaced the input raw data records between $2.5 \cdot 10^4$ to $3 \cdot 10^4$ with the modelled Fourier data, what generated the combined time series mentioned above in the pseudo code (Figure 6a). The dash-lined rectangle represents a forecasting horizon (multistep-ahead prediction) between 03:00 hr of 06-13-1988 year to 03:00 hr 27-02-1990 year (1.71 years).

The performance of the Hybrid Fourier-NAR model revealed that residuals retrieved during the forecasting were lower compared to the residuals of the validation stage (Figure 6a). In this sense, The Fourier input data not only provide the targets (combined time series) for the Neural model, but also gathers the natural variability of the wind speed what allowed reducing the residuals. The results of the standard NAR model (Figure 6b) evidenced that the model could not simulate the wind speed because after several step-ahead predictions the wind speed kept in 3.83 m/s. Accordingly, was evidenced that Hybrid Fourier-NAR model outperformed the NAR model.

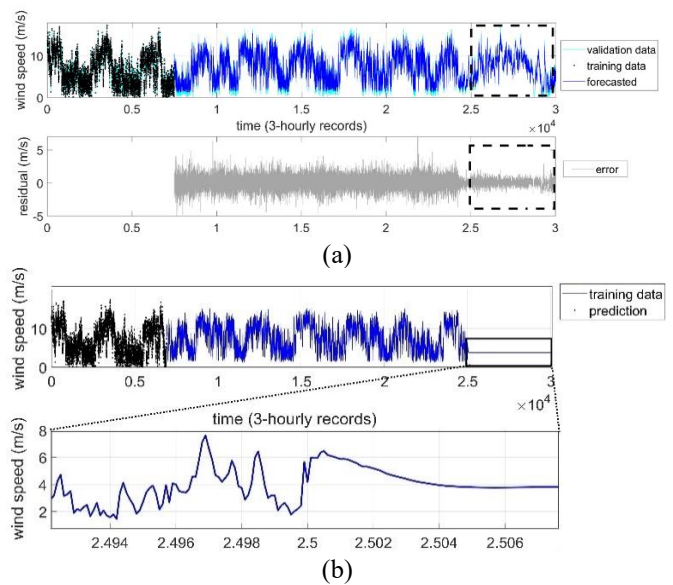


Figure 6. Results of the wind speed forecasted methodology for Barranquilla a) Hybrid Fourier-NAR modelled data and residuals, b) NAR modelled data and zoom over the forecasting period

The Figure 7a shows the validation of the WS forecasting, where the Fourier-NAR model reached a high r -correlation ($r = 0.96$) and a root mean squared error (RMSE) of 0.60 m/s, a low error that is significantly important for the cut-in wind

speed of wind turbines.

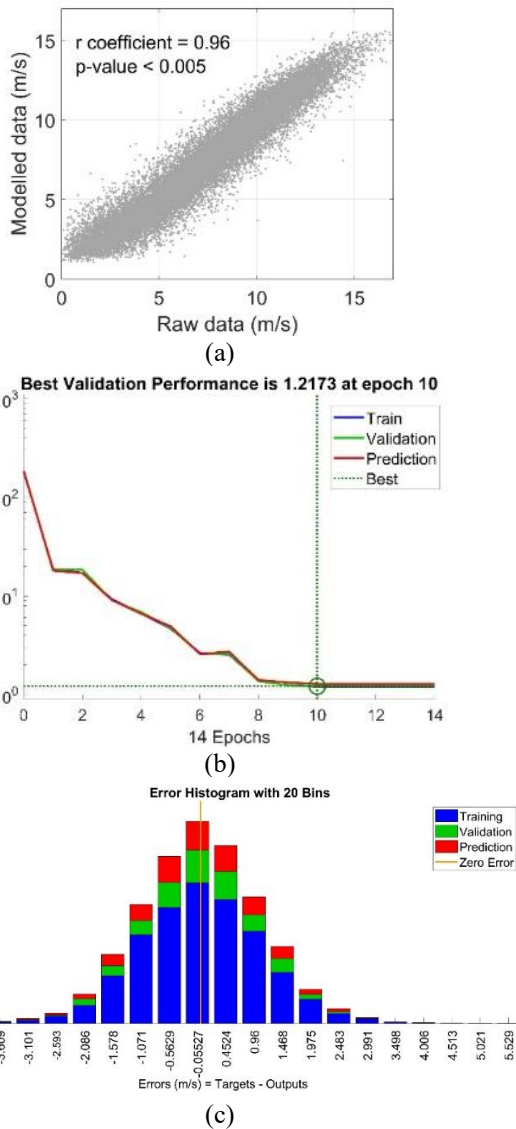


Figure 7. Validation of wind speed results: Fourier-NAR model

The Fourier-NAR model reported a high efficiency because of the low number of achieved epochs Figure 7b. The error distribution of the Fourier-NAR model depicted a positive skew what suggests that model is conservative. Also, was evidenced that the model tends to underestimate rather than overestimating due to the distribution of negative errors (Figure 7c). To increase the r-correlation during the validation of the hybrid Fourier-NAR model, a quality control of the input data (raw time series) could be performed, which consist in removing outlier WS values after a cumulative frequency analysis and the removing of linear-nonlinear trends of the time series. These trends could be generated by induced errors during the recording of WS data, e.g technical problems of WS sensors, or due to the effect of climate-change associated to the global warming. Because Fourier is a numerical approach dependent of sin-cos functions, is proper removing signals that do not belong to the natural behavior of the system. This study recommends removing these trends only for the input data of the Fourier-NAR model, because the training stage of the NAR model requires a raw time series without alterations (step 3a, Figure 2).

Because of the statistical results of the model assessment, the use of Fourier model is proper (Figure 5) because it allowed to provide the target (input) data (1.7 years) for the open loop forecasting (Figure 6a), solving the difficulties of feeding the NAR models with input data with long-term and high-time interval resolution. As was shown in the literature review, the NAR models are good mimics of target (input) time series what means a multistep-back prediction (simulating the past), but when simulating to the future (multistep-ahead prediction), fails because it need inputs (WS) that have not occurred in the real life. In addition, NAR models in close loop mode fails when performing for long time series, as was evidenced in Figure 6b.

After the model assessments, the statistical results demonstrated the accuracy of the Fourier-NAR model to forecast the WS. Table 2 depicts the structure of the NAR model calibrated for Barranquilla city.

Table 2. Parameters and statistical results structure of the calibrated NAR model for Barranquilla

City	Barranquilla			
Time delay	1, 7, 13, 19			
Input weights	0.7310	0.1441	0.0009	-0.0411
Layer weight	1.2632			
Bias	0.0193, -0.0325			
r coefficient	0.96			
p-value	0			
Learning rate	0.25			

A correlation coefficient of 0.96 between the WS forecasted and the data extracted from NARR shows the accuracy of the forecasting process for 1.7 years of time horizon. These results demanded limited computing capacities, which is a further advantage of the NAR model developed.

4. CONCLUSIONS

The hybrid Fourier-NAR model utilized validated Reanalysis data and forecasted accurately the WS at the local scale for 1.7 years of time horizons at 3 hours of the time interval, what may be considered as the longest local wind-speed forecasting at the moment. This approach can be implemented in locations without meteorological stations, which is the case for many locations worldwide, to assess the wind energy potential and define opportunities to exploit wind turbines at the local scale. Given its low computational demand, this method is a viable alternative for forecasting the wind speed at the local scale and thus, to overcome the lack of data precluding the implementation of wind turbines for different locations worldwide.

ACKNOWLEDGMENT

This work is supported by the Universidad Militar Nueva Granada (Project INV-ING 3196).

REFERENCES

[1] British Petroleum, Statistical review of world energy, 2017. <https://www.bp.com/content/dam/bp/business-sites/en/global/corporate/pdfs/news-and->

- insights/speeches/bp-statistical-review-of-world-energy-2017-lamar-mckay.pdf.
- [2] IPCC, Climate Change 2014: Mitigation of climate change, 3. Cambridge University Press, 2014.
- [3] Sawin, K., Sverrisson, J., Seyboth, F., Adib, K., Murdock, R., Lins, H.E., Satzinger, C. (2017). Renewables 2017 Global Status Report.
- [4] International Energy Agency, Renewables 2017. Analysis and forecasts to 2022., 2017. <https://www.iea.org/reports/renewables-2017>.
- [5] Alkhalidi, M.A., Al-Dabbous, S.K., Neelamani, S., Aldashti, H.A. (2019). Wind energy potential at coastal and offshore locations in the state of Kuwait. *Renewable Energy*, 135: 529-539. <https://doi.org/10.1016/j.renene.2018.12.039>
- [6] Wisser, R., Bolinger, M., Heath, G., Keyser, D., Lantz, E., Macknick, J., Millstein, D. (2016). Long-term implications of sustained wind power growth in the United States: Potential benefits and secondary impacts. *Applied Energy*, 179: 146-158. <https://doi.org/10.1016/j.apenergy.2016.06.123>
- [7] Saidur, R., Rahim, N.A., Islam, M.R., Solangi, K.H. (2011). Environmental impact of wind energy. *Renewable and Sustainable Energy Reviews*, 15(5): 2423-2430. <https://doi.org/10.1016/j.rser.2011.02.024>
- [8] Global Wind Energy Council, Global wind energy outlook 2016, 2016. <https://gwec.net/global-wind-energy-outlook-2016/>.
- [9] Rueda-Bayona, J.G., Guzmán, A., Eras, J.J.C., Silva-Casarin, R., Bastidas-Arteaga, E., Horrillo-Caraballo, J. (2019). Renewables energies in Colombia and the opportunity for the offshore wind technology. *Journal of Cleaner Production*, 220: 529-543. <https://doi.org/10.1016/j.jclepro.2019.02.174>
- [10] Perez-Arriaga, I.J. (2011). Managing large scale penetration of intermittent renewables. In MITEI Symposium on Managing Large-Scale Penetration of Intermittent Renewables, Cambridge/USA, 20(4): 2011.
- [11] Jiang, P., Li, C. (2018). Research and application of an innovative combined model based on a modified optimization algorithm for wind speed forecasting. *Measurement*, 124: 395-412. <https://doi.org/10.1016/j.measurement.2018.04.014>
- [12] Sweeney, C., Bessa, R.J., Browell, J., Pinson, P. (2020). The future of forecasting for renewable energy. *Wiley Interdisciplinary Reviews: Energy and Environment*, 9(2): e365. <https://doi.org/10.1002/wene.365>
- [13] Skittides, C., Früh, W.G. (2014). Wind forecasting using principal component analysis. *Renewable Energy*, 69: 365-374. <https://doi.org/10.1016/j.renene.2014.03.068>
- [14] Kavasseri, R.G., Seetharaman, K. (2009). Day-ahead wind speed forecasting using f-ARIMA models. *Renewable Energy*, 34(5): 1388-1393. <https://doi.org/10.1016/j.renene.2008.09.006>
- [15] Wang, J., Song, Y., Liu, F., Hou, R. (2016). Analysis and application of forecasting models in wind power integration: A review of multi-step-ahead wind speed forecasting models. *Renewable and Sustainable Energy Reviews*, 60: 960-981. <https://doi.org/10.1016/j.rser.2016.01.114>
- [16] Jaramillo, O.A., Borja, M.A. (2004). Wind speed analysis in La Ventosa, Mexico: A bimodal probability distribution case. *Renewable Energy*, 29(10): 1613-1630. <https://doi.org/10.1016/j.renene.2004.02.001>
- [17] Segura-Heras, I., Escrivá-Escrivá, G., Alcázar-Ortega, M. (2011). Wind farm electrical power production model for load flow analysis. *Renewable Energy*, 36(3): 1008-1013. <https://doi.org/10.1016/j.renene.2010.09.007>
- [18] Wang, X., Guo, P., Huang, X. (2011). A review of wind power forecasting models. *Energy procedia*, 12: 770-778. <https://doi.org/10.1016/j.egypro.2011.10.103>
- [19] Zhang, Y., Wang, J., Wang, X. (2014). Review on probabilistic forecasting of wind power generation. *Renewable and Sustainable Energy Reviews*, 32: 255-270. <https://doi.org/10.1016/j.rser.2014.01.033>
- [20] Chang, W.Y. (2014). A literature review of wind forecasting methods. *Journal of Power and Energy Engineering*, 2(04): 161. <https://doi.org/10.4236/jpee.2014.24023>
- [21] Guo, W., Wu, G., Liang, B., Xu, T., Chen, X., Yang, Z., Jiang, M. (2016). The influence of surface wave on water exchange in the Bohai Sea. *Continental Shelf Research*, 118: 128-142. <https://doi.org/10.1016/j.csr.2016.02.019>
- [22] Fertig, E. (2019). Simulating subhourly variability of wind power output. *Wind Energy*, 22(10): 1275-1287. <https://doi.org/10.1002/we.2354>
- [23] Duran, M.J., Cros, D., Riquelme, J. (2007). Short-term wind power forecast based on ARX models. *Journal of Energy Engineering*, 133(3): 172-180. [https://doi.org/10.1061/\(ASCE\)0733-9402\(2007\)133:3\(172\)](https://doi.org/10.1061/(ASCE)0733-9402(2007)133:3(172))
- [24] Rueda-bayona, J.G., Cabello, J., Schneider, I. (2018). Wind-speed modelling using fourier analysis and nonlinear autoregressive neural network (NAR). In: F. Giannetti, B.F.; Almeida, C.M.V.B.; Agostinho (Ed.), *Adv. Clean. Prod. Proc. 7th Int. Work.*, Barranquilla, pp. 1-198. http://www.advancesincleanerproduction.net/7th/files/ssoes/6A/8/rueda-bayona_et_al_abstract.pdf (accessed April 8, 2020).
- [25] Eras, J.J.C. (2019). A look to the electricity generation from non-conventional renewable energy sources in Colombia. *Int. J. Energy Econ. Policy*. 9: 15-25. <https://doi.org/10.32479/ijeeep.7108>
- [26] NOAA, NCEP North American Regional Reanalysis: NARR, (2016). <http://www.esrl.noaa.gov/psd/data/gridded/data.narr.html>, accessed on Jan. 5, 2016.
- [27] Soman, S.S., Zareipour, H., Malik, O., Mandal, P. (2010). A review of wind power and wind speed forecasting methods with different time horizons. In *North American Power Symposium 2010*: 1-8. <https://doi.org/10.1109/NAPS.2010.5619586>
- [28] Costa, A., Crespo, A., Navarro, J., Lizcano, G., Madsen, H., Feitosa, E. (2008). A review on the young history of the wind power short-term prediction. *Renewable and Sustainable Energy Reviews*, 12(6): 1725-1744. <https://doi.org/10.1016/j.rser.2007.01.015>
- [29] Liu, H., Duan, Z., Wu, H., Li, Y., Dong, S. (2019). Wind speed forecasting models based on data decomposition, feature selection and group method of data handling network. *Measurement*, 148: 106971. <https://doi.org/10.1016/j.measurement.2019.106971>
- [30] Wang, H.Z., Li, G.Q., Wang, G.B., Peng, J.C., Jiang, H., Liu, Y.T. (2017). Deep learning based ensemble approach for probabilistic wind power forecasting. *Applied Energy*, 188: 56-70. <https://doi.org/10.1016/j.apenergy.2016.11.111>

- [31] Carvalho, D., Rocha, A., Santos, C.S., Pereira, R. (2013). Wind resource modelling in complex terrain using different mesoscale-microscale coupling techniques. *Applied Energy*, 108: 493-504. <https://doi.org/10.1016/j.apenergy.2013.03.074>
- [32] Kotroni, V., Lagouvardos, K., Lykoudis, S. (2014). High-resolution model-based wind atlas for Greece. *Renewable and Sustainable Energy Reviews*, 30: 479-489. <https://doi.org/10.1016/j.rser.2013.10.016>
- [33] Han, Q., Ma, S., Wang, T., Chu, F. (2019). Kernel density estimation model for wind speed probability distribution with applicability to wind energy assessment in China. *Renewable and Sustainable Energy Reviews*, 115: 109387. <https://doi.org/10.1016/j.rser.2019.109387>
- [34] Masseran, N. (2016). Modeling the fluctuations of wind speed data by considering their mean and volatility effects. *Renewable and Sustainable Energy Reviews*, 54: 777-784. <https://doi.org/10.1016/j.rser.2015.10.071>
- [35] Zhao, J., Guo, Z.H., Su, Z.Y., Zhao, Z.Y., Xiao, X., Liu, F. (2016). An improved multi-step forecasting model based on WRF ensembles and creative fuzzy systems for wind speed. *Applied Energy*, 162: 808-826. <https://doi.org/10.1016/j.apenergy.2015.10.145>
- [36] Dhiman, H.S., Deb, D., Guerrero, J.M. (2019). Hybrid machine intelligent SVR variants for wind forecasting and ramp events. *Renewable and Sustainable Energy Reviews*, 108: 369-379. <https://doi.org/10.1016/j.rser.2019.04.002>
- [37] Dong, Q., Sun, Y., Li, P. (2017). A novel forecasting model based on a hybrid processing strategy and an optimized local linear fuzzy neural network to make wind power forecasting: A case study of wind farms in China. *Renewable Energy*, 102: 241-257. <https://doi.org/10.1016/j.renene.2016.10.030>
- [38] Ziel, F., Croonenbroeck, C., Ambach, D. (2016). Forecasting wind power—modeling periodic and non-linear effects under conditional heteroscedasticity. *Applied Energy*, 177: 285-297. <https://doi.org/10.1016/j.apenergy.2016.05.111>
- [39] Meng, A., Ge, J., Yin, H., Chen, S. (2016). Wind speed forecasting based on wavelet packet decomposition and artificial neural networks trained by crisscross optimization algorithm. *Energy Conversion and Management*, 114: 75-88. <https://doi.org/10.1016/j.enconman.2016.02.013>
- [40] Zjavka, L. (2015). Wind speed forecast correction models using polynomial neural networks. *Renewable Energy*, 83: 998-1006. <https://doi.org/10.1016/j.renene.2015.04.054>
- [41] Santamaría-Bonfil, G., Reyes-Ballesteros, A., Gershenson, C. (2016). Wind speed forecasting for wind farms: A method based on support vector regression. *Renewable Energy*, 85: 790-809. <https://doi.org/10.1016/j.renene.2015.07.004>
- [42] Doucoure, B., Agbossou, K., Cardenas, A. (2016). Time series prediction using artificial wavelet neural network and multi-resolution analysis: Application to wind speed data. *Renewable Energy*, 92: 202-211. <https://doi.org/10.1016/j.renene.2016.02.003>
- [43] Zendeheboudi, A., Baseer, M.A., Saidur, R. (2018). Application of support vector machine models for forecasting solar and wind energy resources: A review. *Journal of Cleaner Production*, 199: 272-285. <https://doi.org/10.1016/j.jclepro.2018.07.164>
- [44] Barbounis, T.G., Theocharis, J.B. (2006). Locally recurrent neural networks for long-term wind speed and power prediction. *Neurocomputing*, 69(4-6): 466-496. <https://doi.org/10.1016/j.neucom.2005.02.003>
- [45] Amjady, N., Keynia, F., Zareipour, H. (2011). Short-term wind power forecasting using ridgelet neural network. *Electric Power Systems Research*, 81(12): 2099-2107. <https://doi.org/10.1016/j.epsr.2011.08.007>
- [46] Blonbou, R. (2011). Very short-term wind power forecasting with neural networks and adaptive Bayesian learning. *Renewable Energy*, 36(3): 1118-1124. <https://doi.org/10.1016/j.renene.2010.08.026>
- [47] Azad, H.B., Mekhilef, S., Ganapathy, V.G. (2014). Long-term wind speed forecasting and general pattern recognition using neural networks. *IEEE Transactions on Sustainable Energy*, 5(2): 546-553. <https://doi.org/10.1109/TSTE.2014.2300150>
- [48] Xiao, L., Wang, J., Dong, Y., Wu, J. (2015). Combined forecasting models for wind energy forecasting: A case study in China. *Renewable and Sustainable Energy Reviews*, 44: 271-288. <https://doi.org/10.1016/j.rser.2014.12.012>
- [49] Wang, J., Hu, J., Ma, K., Zhang, Y. (2015). A self-adaptive hybrid approach for wind speed forecasting. *Renewable Energy*, 78: 374-385. <https://doi.org/10.1016/j.renene.2014.12.074>
- [50] Carpinone, A., Giorgio, M., Langella, R., Testa, A. (2015). Markov chain modeling for very-short-term wind power forecasting. *Electric Power Systems Research*, 122: 152-158. <https://doi.org/10.1016/j.epsr.2014.12.025>
- [51] Liu, H., Tian, H.Q., Liang, X.F., Li, Y.F. (2015). Wind speed forecasting approach using secondary decomposition algorithm and Elman neural networks. *Applied Energy*, 157: 183-194. <https://doi.org/10.1016/j.apenergy.2015.08.014>
- [52] Shrivastava, N.A., Lohia, K., Panigrahi, B.K. (2016). A multiobjective framework for wind speed prediction interval forecasts. *Renewable Energy*, 87: 903-910. <https://doi.org/10.1016/j.renene.2015.08.038>
- [53] Zhao, Y., Ye, L., Li, Z., Song, X., Lang, Y., Su, J. (2016). A novel bidirectional mechanism based on time series model for wind power forecasting. *Applied Energy*, 177: 793-803. <https://doi.org/10.1016/j.apenergy.2016.03.096>
- [54] Zhao, W., Wei, Y.M., Su, Z. (2016). One day ahead wind speed forecasting: A resampling-based approach. *Applied Energy*, 178: 886-901. <https://doi.org/10.1016/j.apenergy.2016.06.098>
- [55] Zhang, C., Wei, H., Zhao, J., Liu, T., Zhu, T., Zhang, K. (2016). Short-term wind speed forecasting using empirical mode decomposition and feature selection. *Renewable Energy*, 96: 727-737. <https://doi.org/10.1016/j.renene.2016.05.023>
- [56] Wang, S., Zhang, N., Wu, L., Wang, Y. (2016). Wind speed forecasting based on the hybrid ensemble empirical mode decomposition and GA-BP neural network method. *Renewable Energy*, 94: 629-636. <https://doi.org/10.1016/j.renene.2016.03.103>
- [57] Lydia, M., Kumar, S.S., Selvakumar, A.I., Kumar, G.E.P. (2016). Linear and non-linear autoregressive models for short-term wind speed forecasting. *Energy Conversion and Management*, 112: 115-124. <https://doi.org/10.1016/j.enconman.2016.01.007>

- [58] Jiang, P., Li, P. (2017). Research and application of a new hybrid wind speed forecasting model on BSO algorithm. *Journal of Energy Engineering*, 143(1): 04016019. [https://doi.org/10.1061/\(ASCE\)EY.1943-7897.0000362](https://doi.org/10.1061/(ASCE)EY.1943-7897.0000362)
- [59] Beale, M., Hagan, M., Demuth, H. (2020). *Deep Learning Toolbox™ Getting Started Guide*. The MathWorks, Inc.: Natick, MA, USA.
- [60] Rockmore, D.N. (2000). The FFT: An algorithm the whole family can use. *Computing in Science & Engineering*, 2(1): 60-64. <https://doi.org/10.1109/5992.814659>
- [61] Chu, E., George, A. (1999). *Inside the FFT Black Box: Serial and Parallel Fast Fourier Transform Algorithms*. CRC Press.
- [62] Rueda Bayona, J.G., Elles Pérez, C.J., Sánchez Cotte, E.H., González Ariza, Á.L., Rivillas Ospina, G.D. (2016). Identificación de patrones de variabilidad climática a partir de análisis de componentes principales, Fourier y clúster k-medias. *Tecnura*, 20(50): 55-68. <https://doi.org/10.14483/udistrital.jour.tecnura.2016.4.a04>
- [63] Brigham, E. (1988). *Fast Fourier Transform and Its Applications*.
- [64] Zonst, A. (2000). *Understanding the FFT*, 2nd ed., 2000.
- [65] Hewitt, E., Hewitt, R. (1979). *Archive for History of Exact Sciences: An Episode in Fourier Analysis*.
- [66] Rasmussen, H.O. (1993). The wavelet Gibbs phenomenon. *Wavelets, Fractals, and Fourier Transforms* (M. Farge, JCR Hunt, and JC Vassilicos, eds.), 123-142.
- [67] Kelly, S. (1995). *Gibbs Phenomenon for Wavelets: Applied and Computational Harmonic Analysis*, 1st ed., 1995.
- [68] Chan, R.W., Yuen, J.K., Lee, E.W., Arashpour, M. (2015). Application of Nonlinear-Autoregressive-Exogenous model to predict the hysteretic behaviour of passive control systems. *Engineering Structures*, 85: 1-10. <https://doi.org/10.1016/j.engstruct.2014.12.007>
- [69] Widrow, B., Hoff, M.E. (1989). Adaptive switching circuits, in: *Wescon Conf. Rec.*, 1989.
- [70] NOAA, NCEP North American Regional Reanalysis: NARR, (2016).